

# Capacitively Coupled Electrode Antenna: A Practical Solution for Biomedical Implants

A. Khaleghi<sup>1,2</sup>, I. Balasingham<sup>1,2</sup>, Senior Member, IEEE

<sup>1</sup>Norwegian University of Science and Technology, NTNU, Trondheim, Norway

<sup>2</sup>Oslo University Hospital, OUH, Oslo, Norway

Email: ali.khaleghi@ntnu.no

**Abstract-** A capacitively coupled electrode antenna is proposed for use in medical implants. The antenna involves the conductivity of the biological medium and extends the applied RF electric signal to the conductive biological medium, thus the antenna virtual size increase that results in higher radiation efficiency compared to the similar size physical antennas. The antenna is self-matched or can be easily matched to a 50-ohm source impedance and provides ultra-wideband impedance matching that makes it less sensitive to the variations of the surrounded biological tissues. The proposed antenna occupies a minimal volume, which is a requirement for the implants. The physical structure of the antenna is similar to the contact electrodes but uses a capacitive coupling gap to the medium to increase radiation efficiency and reduce the specific absorption rate (SAR). A sample antenna at 403 MHz is designed and compared to the ideal conventional dipole and loop geometries.

*Keywords:* Antennas, wireless communications, Implant, medical applications, electrode antenna

## I. Introduction

Medical implants have growing use in collecting health information of patients, and wireless communication technology helps to remove the cables from implants for safer sensing, diagnosis and treatments. Examples of market available implant devices are cardiac pacemaker, leadless cardiac pacemaker, wireless capsule endoscopy, glucose implant sensors and brain stimulators. The implant size is the major concern that can affect the field of application. The antenna is a part of a communication system that plays a crucial rule on wireless data transfer in which the antenna efficiency, integration, compatibility and radiation safety are the major essential factors. Due to the implant size limitations, antenna integration with medical implants faces some challenges. First, the antenna radiation efficiency and the input impedance are mainly governed by the antenna's electrical size in which poor radiation efficiency and non-tunable impedance are the major concerns. Second, the biological tissues contain a high amount of minerals and ionic material in which the material conductivity performs as a loss to the electromagnetic signal in transmission through the medium, also the high permittivity of the tissues, due to the water contents, results in the antenna near field confinement to the proximity of the device. Also, for wireless communication with off-body devices, the mismatch between the tissue medium and free-space

results in wave reflections on the surface and thus reduced EM radiations to the external medium occurs.

The antenna miniaturization techniques for implant devices follow the same design concept applied in free space based on the topology and material [1]. The topology is based on space-filling curves (meander, fractal), engineered ground plane, reactive loading, slow-wave using periodic structures and antenna distributed loading. All these techniques provide a substantial trade-off between size reduction and bandwidth, efficiency and gain. Lump elements can be used to reduce the antenna size; however, it can add ohmic loss and the parasitic effects cause self-resonance that leads to efficiency loss, in addition, using lump elements is not practical in RF. Using the miniaturized antennas in the biological implant or in the vicinity of the biological tissues can significantly damage the antenna Q-factor and drops the radiation efficiency by adding the loss resistance to the antenna equivalent circuit. Thus, the antenna matching bandwidth can be increased. Though the wide bandwidth might be beneficial to support high data rates but the efficiency drop is the primary concern since generating the power using implant battery resources is expensive. Compared to the free space, the complex permittivity of the biological tissues with high real permittivity value confines the antenna near-field very close to the antenna structure and the material conductivity dissipates the near-field. Thus the biologically embedded antenna indicates very poor efficiency even by considering the natural loss associated with the wave transmission through the lossy medium.

Different antenna geometries and configurations have been proposed for implant usage. Some examples are the spiral antenna [2], meander dipole antenna [3,4], and conformal antennas [4,5,7]. The main objective in these designs is geometry and size that must satisfy the impedance matching for efficient power delivery from the source and sufficient bandwidth to support high data rate, in addition, to omnidirectional and dual polar radiation patterns with small specific absorption rate (SAR) are the design criteria. The proposed antennas in [3-5] use the general geometry of dipole antennas with different shapes for reducing the resonance length of the antenna. The antennas in [2, 6] use loop antenna geometry for improved efficiency and reduced SAR value due to the nature of EM wave propagation with the loop geometry in the biological

tissues. Among the proposed antennas, some are designed to have a conformal geometry to save the space for the electronics [4,5,7] and some use a part of the implant space [2,3,7] for integrations. The analytical calculations of tiny conceptual dipole and loop antennas in biological tissues is provided in [8,9]. However, the practical considerations were not the study case.

In this paper, we consider a small antenna of a maximum length of 10 mm operating in the Medical Implant Communication System (MICS) frequency band at 403 MHz. The antenna physical length compared to wavelength ( $\lambda$ ) in free space is  $0.0067\lambda$ . We provide the full-wave antenna simulations for two canonical antennas of dipole and loop in the biological mediums and compare it to our suggested capacitive coupled electrode antenna (CCEA).

## II. Simulation models

Numerical computations are used to calculate the performance of a tissue embedded antenna. First, two conceptual antennas: dipole and loop, are used in the simulations, followed by the simulation of the CCEA. For the simplicity and reproducibility of the results, we consider a spherical muscle tissue model of the radius ( $R_s$ ). The antennas are embedded at the center of the muscle sphere in a vacuum sphere of the radius ( $r=5$  mm). Frequency domain (FD) solver in CST MWS is used for computations because of the small size of the antennas compared to the wavelength, in which fast and accurate results can be obtained in FD compared to the time domain (TD) solver in CST MWS. Some sample simulations are validated by TD solver in CST to verify the FD results. The simulation frequency is at 403 MHz. The antenna parameters include impedance, radiation efficiency, and the SAR are calculated. Figure. 1 shows the simulation model with different antennas embedded in the muscle sphere. The electromagnetic material property of biological tissues is modeled using the Cole-Cole model based on the measurements provided by Gabriel [10]. Figure. 2 shows the frequency-dependent permittivity and conductivity for some sample biological tissues, including the muscle for the frequency range of 300-600 MHz. The permittivity is frequency-dependent and varies for different tissues. The material conductivity increases with frequency increment. For the muscle tissue at 403 MHz,  $\epsilon=57-j36$ ,  $\sigma=0.79$  S/m. Due to the complex permittivity and thus the conductivity of the material, the wave propagation in the complex medium observes additional electric field decay than the decay related to the spherical wave expansion. In addition, the large real part of the permittivity confines the electric field to the source proximity, and thus additional loss is observed. The biological tissues in the microwave range are mainly diamagnetic, and the permeability is a real value of  $\mu_r=1$ . Therefore, the nature of the generated field by the antenna inside the biological tissues can affect the wave

propagation loss in the medium. The magnetic field is preferred for energy coupling and power transfer in biological tissues. However, there is not any known pure magnetic source

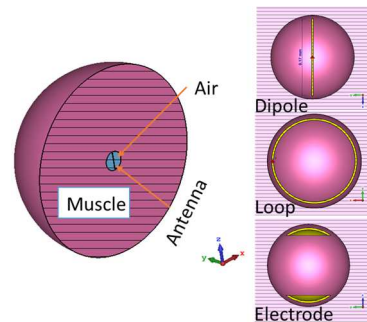


Fig.1 Simulation scenarios of dipole, loop, and electrode antennas in spherical muscle tissue of radius  $R$ ; The antennas are placed inside the air sphere of diameter 10 mm.

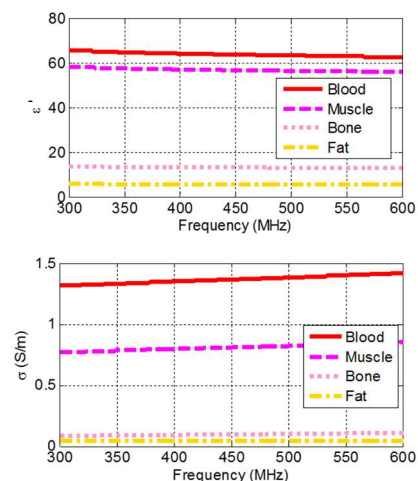


Fig.2 Real part of permittivity and conductivity of Muscle, Blood, Fat, and Bone tissues versus frequency

that can be implemented in such a medium. The magnetic source can be realized by using an electric loop at the frequencies that the loop length is extremely small compared to the wavelength. In these frequencies, the loop antenna input resistance is very small, so the circuit accepts high current flow, and a strong magnetic field is created. By increasing the loop antenna length, the input resistance of the metal loop is governed by the radiation resistance, and the antenna performs as an electric antenna. The loop antenna impedance curves define the region that the loop can be considered as a magnetic antenna or radiating element.

### A. Dipole and loop in muscle tissue

Simulations of the loop and dipole antennas are conducted using FD solver in CST. The antennas are constructed from lossy Aluminum wire ( $\sigma=3.56 \times 10^7$ ) of diameter is 0.2 mm. The loop has a constant gap of 0.5

mm to the surrounded muscle tissue, and the dipole tips have a 0.5 mm gap to the muscle. Muscle sphere of radius ( $R_s = 10$  cm) is considered. Table 1 summarizes the simulated antenna impedances and the far-field radiation efficiency at 403 MHz. The radiation efficiency does not consider the antenna mismatch effects, i.e., it assumes perfect impedance matching,

Table 1. Simulated results of dipole, loop and electrode antennas in muscle sphere of  $R_s = 100$  mm at 403 MHz

Antenna Type	Z ( $\Omega$ )	Rad. eff. (dB)	SAR (10g) W/K g	Q-factor	10 dB BW (MHz)
Dipole (air)	0.057-j8296	-3.37	-	-	-
Dipole (Muscle)	9.9-j7609	-34.8	26.6	806	0.35
Loop (air)	0.34+j60	-28	-	-	-
Loop (Muscle)	0.85+j60	-28.6	7.0	72	3.5
CCEA	30+j0	-34.5	47.5	1.3	100

and includes the loss in the antenna metal structure (Aluminum) and the loss in the muscle medium. For the sake of comparison, the antenna parameters are also simulated in air and listed in the table.

The short dipole impedance in free space is  $Z_d = 0.057 - j8296$ , and it has very small input resistance in which is mainly associated with the conductor loss, and the antenna is highly capacitive. By placing the short dipole in the muscle tissue within the air sphere of  $R_a = 10.5$  mm, the embedded dipole input impedance becomes  $Z_{de} = 9.9 - j7609 \Omega$ , where the antenna ohmic resistance increased to  $9.9 \Omega$ , due to the antenna near-field loading with the muscle tissues, especially in the antenna tips where the distance to the muscle is minimal (0.5mm) compared to the center. The embedded dipole is highly capacitive both in free space and in the muscle tissue that makes it almost impossible to provide practical low loss matching to a  $50 \Omega$  load. The imaginary part of the impedance has small variations (about 8%) due to the change from air to the muscle. The far field radiation efficiency of the dipole is calculated in free space and inside the muscle sphere of radius 100 mm. The radiation efficiency is reduced by 31.4 dB for the muscle embedded antenna due to the antenna near field loading by the muscle and the wave propagation loss in the muscle tissue. The muscle embedded antenna is simulated for different sizes ( $R_s$ ) of the muscle. It is observed that the dipole antenna impedance is almost constant for all the muscle sizes. Figure 3 shows the radiation efficiency of dipole versus  $R_s$ . As shown, by increasing the muscle radius from  $R_s = 20$  to 70 mm, the embedded antenna efficiency increases with the rate of 2.7 dB/cm because the tissue is a part of the radiating element and the antenna effective size increases

that results to the efficiency improvement and radiation from the whole lossy sphere. However, for  $R_s > 70$  mm, the material loss becomes dominant compared to the size factor and the efficiency remains constant for  $R_s = 70$  to 100 mm, for  $R_s > 100$  mm, the efficiency reduces gradually by 1.38 dB/cm due to the material loss. The calculated SAR (10g) of the dipole is 26.6 W/kg for the accepted power of 1 W. The calculated Q-factor of the dipole is about 806, which is very high and it is almost impossible to match the antenna to a  $50 \Omega$  source impedance without significant loss. The potential bandwidth of the antenna is about 0.35 MHz.

The loop antenna simulation in free space and inside the muscle sphere is performed. The antenna impedance in free space is  $Z_L = 0.34 + j60$  and in the muscle is  $Z_{Le} = 0.85 + j60$ . The antenna resistance in free space is small and the biological tissues increase the resistance slightly. The imaginary part is inductive and is the same for both air and muscle. Thus, the small loop impedance is mainly governed by the antenna itself rather than the surrounded medium. The antenna radiation efficiency in free space at 403 MHz is -28 dB, and is reduced by 0.6 dB in the muscle for  $R_s = 100$  mm. The small radiation efficiency in free space and the muscle is due to the conductor loss. However, as the loop antenna length ( $L = 2\pi r = 31$  mm  $= 0.04 \lambda$ ) is very small compared to the wavelength, it performs as a magnetic antenna in which the magnetic field loss is smaller in the biological tissues compared to the electric counterpart. Figure 3 shows the radiation efficiency of the loop for different

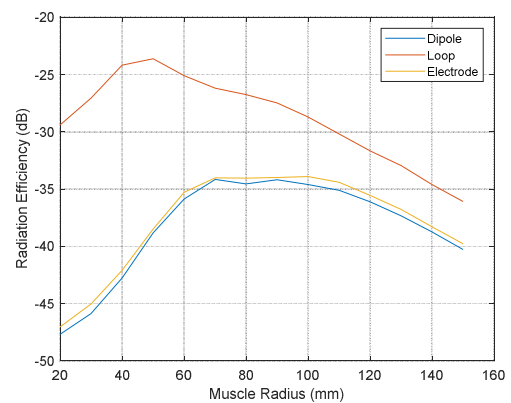


Fig.3 Radiation efficiency of muscle embedded dipole, loop and electrode antenna versus muscle size.

muscle size ( $R_s$ ) by assuming perfect matching. As shown, loop has significantly higher efficiency than the dipole for small muscle size. By increasing  $R_s$ , the antenna efficiency increases up to -24 dB for  $R_s = 50$  mm. The muscle embedded antenna efficiency is higher than the loop in free space by about 5 dB. The reason is the increased embedded antenna physical size that augments the radiation efficiency without significant loss of the magnetic field in the tissues. However, for  $R_s$  greater than

50 mm the efficiency reduces by 1.25 dB/cm. This loss is related to the electric field loss decay in the muscle tissue, in which it shows that the loop is not a pure magnetic radiator. However, the loop has a significant magnetic near field with less loss by the tissues that make the loop, conceptually, appropriate for superficial implant usage. The computed SAR (10g) of the loop is 7.0 W/Kg for 1W of the accepted power. The SAR is much smaller than the dipole antenna; however, the SAR does not count the heat effect that is generated in the loop wire, which should be high due to the low antenna resistance. The loop antenna has very low resistance ( $0.85\Omega$ ) in which the current flow in the loop becomes significant and the heating in the matching circuit and wire structure becomes problematic. To retain the efficiency of the loop high Q-factor discrete elements are required for matching in which it is not easy to develop at 403 MHz, and the antenna impedance is very sensitive to the changes in the matching components caused by the heat. The Q-factor of the loop is 72 and the potential bandwidth without loss is 3.5 MHz. Therefore, adding some loss to the loop is required to reduce the Q factor on the exchange of the efficiency loss. This can be done by coating the loop with ferrite material; however, the use of magnetic material is not allowed for the implants due to magnetic compatibility requirements for MRI medical imaging devices. Thus, the impedance can be increased by using lossy metal; for instance, by reducing conductivity by factors of 10, 100, and 1000, the antenna input resistance increases to 1.58, 3.9, and 11.2  $\Omega$ , but the radiation efficiency becomes -31, -35, -39 dB, respectively, for  $R_s=100$  mm at 403 MHz.

In reference to Figure 3, the comparison of the dipole and loop antennas indicates about 4 dB better performance of the loop for deep implants,  $R>120$  mm, and significant ( $>10$  dB) efficiency improvement for superficial implants ( $R<60$  mm) without considering the antenna matching issues. From the practical point of view, it is difficult to match the small loop and dipole to a 50  $\Omega$  source without adding additional losses in which the antenna efficiency reduces significantly, the antennas become sensitive to the matching components, the surrounded biological tissues and the proximity electronics.

## B. Electrode antenna

Electrode antennas are used for intra-body communications (IBC) in which the galvanic property of biological tissues is used to conduct signals in low-frequency region kHz and lower MHz. Using electrode antennas in RF is new that is considered in this paper. We use a pair of metal plates with a given surface area and apply an air gap to couple RF signal to the biological medium. Thus, the electrode has not any contact with the tissues that is a feature regarding the bio-compatibility of the metallic material. Figure 4 shows a simple electrode antenna configuration. The electrode surface area, the distance between the electrodes and the coupling gap

defines the antenna impedance. To compare the electrode antenna performance with loop and dipole configurations, the previous simulation setup is considered. Two cuts of sphere shape electrodes are used with a separation distance of 10 mm, a gap of 0.2 mm is used between the muscle and the electrodes.

The gap is used to prevent direct contact of the metal with biological tissues. The antenna is simulated using FD solver in CST. The antenna has a resonance at 403 MHz with  $Z=30+j0 \Omega$ . The antenna radiation efficiency for  $R_s=100$  mm is -34.5 dB at 403 MHz. The radiation efficiency for different size of the muscle sphere is shown in Fig. 3, the efficiency increase with the muscle size for  $R_s < 60$  mm, it is almost constant for  $R_s=60$  to 100 mm, and reduces gradually with 1.3 dB/cm for  $R_s>120$  and the efficiency follows the same trend as the dipole antenna. The main difference with the dipole is that the antenna has a resonance at 403 MHz with  $R_{in}=30 \Omega$ , and it can be easily matched without any loss to a 50  $\Omega$  source, or it can be used without matching circuit. The main feature of the

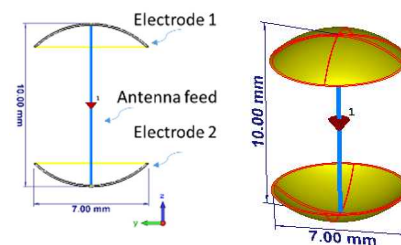


Fig.4 CCEA model with two electrodes in muscle and a gap of 0.2 mm to the medium, a) cut plane b) 3D model

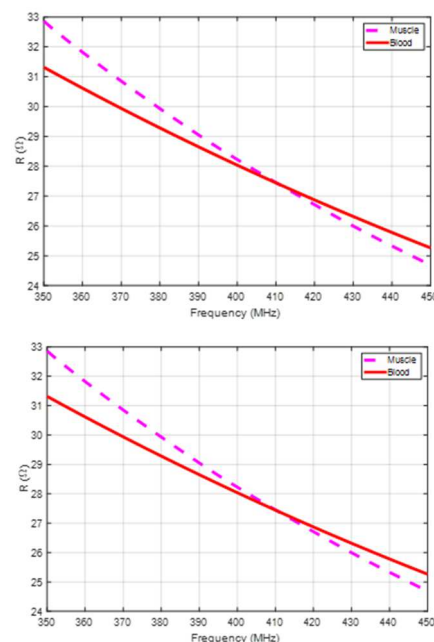


Fig.5 Impedance of the CCEA in muscle and blood tissues.

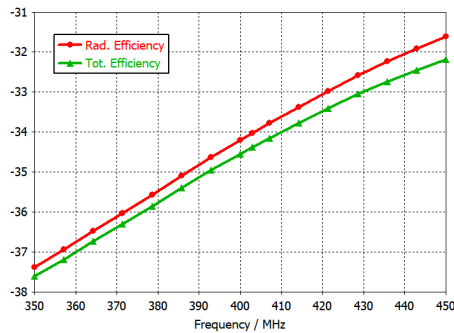


Fig.6 Radiation efficiency and total efficiency of CCEA in muscle versus frequency (without matching)

antenna is that it uses the distributed conductivity of the biological tissues for the matching purposes. The antenna has a very low Q-factor of 1.3 and it can provide a bandwidth of 100 MHz at 403 MHz. The ultra-wideband feature of the antenna makes it appropriate to operate in different conductive tissues such as muscle, blood, intestine and brain with acceptable variations in the impedance also with the scattering parameter below 10 dB without matching. However, the antenna impedance performance in dry tissues such as fat or bone is not such efficient and requires antenna matching. Fig.5 shows the antenna impedance parameters versus frequency inside blood and muscle tissues, in which small variations are visible. The radiation efficiency and the total efficiency of the muscle embedded antenna versus frequency without matching is shown in Fig.6. As shown, the total efficiency of CCEA has about 0.5 dB degradation compared to the radiation efficiency without using antenna matching for the whole bandwidth of 100 MHz (350-450 MHz).

### III. Conclusion

Small loop and dipole antennas are compared for implant applications. It is shown that both antennas have inherent limitations for practical use. Capacitively coupled electrode antenna (CCEA) is proposed as a general solution for RF implantable antennas. The antenna has two electrodes with a separation distance and a given electrode surface that couples the RF signal to the conductive medium in biological implants. A coupling gap is used to prevent direct contact with the tissues and provide antenna matching by adding an equivalent capacitive element to the antenna circuit. The antenna uses the distributed conductivity of the biological tissues to provide ultra-wideband matching without using any extra matching circuit. Also, the biological tissues generate a lossy conductive loop between the electrodes through the medium in which it perform as an inductor and removes the capacitive nature of the antenna. The high permittivity of the tissues is used to miniaturize the antenna size. The antenna can be integrated into the shell of an implant device and provides high efficiency as an

ideal matched dipole and occupies a very small volume. The electronics and other circuits do not influence the antenna characteristics because of the low Q antenna. The performance of CCEA is compared to the loop and dipole antennas in which it shows 5 dB worse performance than an ideal loop in deep implants, but CCEA is a practical implant antenna solution with a wide tuning flexibility. The antenna SAR (10g) is 47.5 W/kg, for accepted power of 1W, where we can apply 41 mW (16 dBm) for SAR (10g) of 2 W/kg. The power is much higher than enough for providing long-range communication from implant to a remote hub.

### Acknowledgment

The work has been supported by the Research Council of Norway projects "Wireless In-body Sensor and Actuator Networks (WinNow), grant no. 270957 and Communication Theoretical Foundation of Wireless Nanonetworks (CIRCLE), grant no. 287112.

### References

- [1] M. Fallahpour and R. Zoughi, "Antenna Miniaturization Techniques: A Review of Topology- and Material-Based Methods," *IEEE Antennas Propag. Mag.*, vol. 60, no. 1, pp. 38–50, Feb. 2018.
- [2] S. I. Kwak, K. Chang, and Y. J. Yoon, "Small spiral antenna for wideband capsule endoscope system," *Electron. Lett.*, vol. 42, no. 23, pp. 1328–1329, 2006.
- [3] Y. Li, Y. X. Guo, and S. Xiao, "Orientation Insensitive Antenna with Polarization Diversity for Wireless Capsule Endoscope System," *IEEE Trans. Antennas Propag.*, vol. 65, no. 7, pp. 3738–3743, Jul. 2017.
- [4] H. Yu et al., "Printed capsule antenna for medication compliance monitoring," *Electron. Lett.*, vol. 43, no. 22, pp. 1179–1181, 2007.
- [5] P. M. Izdebski, H. Rajagopalan, and Y. Rahmat-Samii, "Conformal ingestible capsule antenna: A novel chandelier meandered design," *IEEE Trans. Antennas Propag.*, vol. 57, no. 4 PART. 1, pp. 900–909, 2009.
- [6] T. Yousefi and R. E. Diaz, "Pushing the limits of radiofrequency (RF) neuronal telemetry," *Sci. Rep.*, vol. 5, pp. 1–16, 2015.
- [7] A. Khaleghi, A. Hasanvand, and I. Balasingham, "Radio frequency backscatter communication for high data rate deep implants," *IEEE Trans. Microw. Theory Tech.*, vol. 67, no. 3, pp. 1093–1106, 2019.
- [8] A. K. Skrivervik, M. Bosiljevac and Z. Sipus, "Electrically small antenna design: from mobile phones to implanted sensors," 2019 13th European Conference on Antennas and Propagation (EuCAP), Krakow, Poland, 2019, pp. 1-5.
- [9] A. K. Skrivervik, M. Bosiljevac and Z. Sipus, "Fundamental Limits for Implanted Antennas: Maximum Power Density Reaching Free Space," in *IEEE Transactions on Antennas and Propagation*, vol. 67, no. 8, pp. 4978–4988, Aug. 2019.
- [10] S. Gabriel, R. W. Lau, and C. Gabriel, "The dielectric properties of biological tissues: II. Measurements in the frequency range 10 Hz to 20 GHz," *Phys. Med. Biol.*, vol. 41, no. 11, pp. 2251–2269, Nov. 1996.